

A topological signature of multipartite entanglement

F. Lingua^{†,1,*} W. Wang (王巍)^{†,2} L. Shpani,¹ and B. Capogrosso-Sansone¹

¹*Department of Physics, Clark University, Worcester, Massachusetts 01610, USA*

²*Max Planck Institute for the Physics of Complex Systems, Nöthnitzer Str. 38, 01187 Dresden, Germany*

[†]*These authors contribute equally to the work.*

(Dated: December 5, 2019)

In this manuscript, we present a proposal to relate topological structure of worldline configurations to multipartite entanglement. Configurations result from the path-integral formulation of the density matrix in the limit of zero temperature. We consider hard-core bosons for which configurations, i.e. collections of particle paths, can be seen as geometric braids with a certain topological structure. We propose that properties of worldline configurations may realize a comprehensive deciphering of multipartite entanglement. By means of Monte Carlo calculations, we study checkerboard, stripe, valence-bond solids, \mathbb{Z}_2 topologically ordered spin liquid, and superfluid phase. We find that each ground-state is characterized by a certain ‘topological spectrum’ which can be used to differentiate among different ground-states.

Introduction Multipartite entanglement describes the complex quantum correlations among different parties involved in a many-body system. Its understanding and characterization have been a fascinating yet challenging task that physicists have been actively pursuing in recent years [1–20]. Signatures of entanglement, e.g. entanglement entropy, entanglement spectrum, topological entanglement entropy, concurrence, quantum Fisher information, entanglement witnesses, have been successfully used to quantify entanglement, characterize fully inseparable states [6] and genuine multiparticle entanglement [7, 8], study quantum phases and transitions [5, 9–19] etc. The majority of these characterizations refer to the entanglement between two partitions of the original system. While successful, this ‘coarse-grained’ approach inevitably gives a reductive view of the complex quantum correlations inherent to a many-body quantum state which cannot be written as a simple product state [21].

To get a sense of this complexity, let us consider three simple examples of a superposition of 4-qubits which possess very different entanglement properties: $|\phi_1\rangle = |0111\rangle + |1011\rangle + |1101\rangle + |1110\rangle$, is a W-state which is a genuine 4-qubit multipartite entangled state; $|\phi_2\rangle = |0111\rangle + |1011\rangle + |1110\rangle = (|01_1\rangle + |10_1\rangle + |11_0\rangle) \otimes |1\rangle$ is not a genuine 4-qubit multipartite entangled state, but rather a genuine 3-qubit multipartite entangled state; and $|\phi_3\rangle = |1000\rangle + |1001\rangle + |1010\rangle + |1011\rangle = |10_ \rangle \otimes (|0\rangle + |1\rangle) \otimes (|0\rangle + |1\rangle)$ is not entangled. These simple examples already suggest that quantum correlations manifest themselves as a complicated arrangement of mutual information shared among parties. It is easy to see that the complexity of entanglement will increase significantly with increasing number of qubits [22]. This ‘yarn bundle’ of shared information is highly non-trivial and, though in recent years methods such as quantum Fisher information [17–19] and tensor network states [23–25] have succeeded in studying multipartite entanglement of certain states, to date, a satisfactory systematic approach to study the structure behind this complicated arrangement

of information is lacking [26].

Typical examples of multipartite entangled states are ground-states of many-body interacting quantum systems. Here, we show that topological structure of worldline configurations may be used to differentiate ground-states of different quantum phases (with different multipartite entanglement properties). The approach is based on Feynman path-integral formulation of the density matrix [27] in the limit of zero temperature. Within this framework, each quantum particle is mapped onto a *classical* trajectory (worldline) in space-imaginary time τ , so that the quantum system is now described in terms of collections of worldlines, i.e. worldline configurations. We propose that the topological structure of worldline configurations, which describes certain classical correlations among worldlines, may be related to certain aspects of multipartite entanglement. In other words, we propose to look at multipartite entanglement through the ‘lens’ of the topological structure of worldline configurations. The proposed approach can be readily implemented within path-integral quantum Monte Carlo. In the following, we provide a formal justification for this proposal and we support it by numerically showing that characterizing worldline configurations in terms of the simplest topological invariant is an effective way to *differentiate* among ground-states with different multipartite entanglement. A more systematic study of topological and geometrical properties of configurations and how they relate to entanglement will be the object of future investigations. In the past, researchers have studied the relationship between braids, knots and entanglement in [28, 29]. We believe pursuing this direction can provide a useful perspective to investigate multipartite entanglement.

Topological structure of worldline configurations and ground-state

According to the imaginary-time path-integral formulation of the density matrix, properties of ground-state $|\Psi\rangle$, as determined by $c_\alpha = \langle \alpha | \Psi \rangle$ ($|\alpha\rangle = |..n_i.. \rangle$, $n_i = 0, 1$ is the occupation at site i), are completely encoded in the

integrals

$$\langle \alpha | \Psi \rangle \langle \Psi | \alpha \rangle = \lim_{\beta \rightarrow \infty} \langle \alpha | \frac{e^{-\beta H}}{\mathcal{Z}_\beta} | \alpha \rangle = \lim_{\beta \rightarrow \infty} \int_{\phi \in \mathcal{C}_\alpha} \frac{\omega_\phi}{\mathcal{Z}_\beta}, \quad (1)$$

with $\omega_\phi \propto \langle \alpha | H_1(\tau_1) | \alpha_1 \rangle \cdots \langle \alpha_{n-1} | H_1(\beta) | \alpha \rangle$ the weight of configuration ϕ and H_1 the off-diagonal part of the hamiltonian (see Supplemental Material for details). Note that, for $c_\alpha \geq 0$, ground-state properties, such as entanglement and quantum correlations, can be equivalently inferred from $\{\omega_\phi\}$ rather than $\{c_\alpha\}$.

Let us consider a worldline configuration ϕ as specified by the sequence of imaginary time instants $0 < \tau_1 < \dots < \tau_{n-1} < \beta$ and corresponding Fock states $\{|\alpha\rangle, |\alpha_1\rangle, \dots, |\alpha_{n-1}\rangle, |\alpha\rangle\}$. Expectation values entering ω_ϕ are nonzero, i.e. $\langle \alpha_m | H_1(\tau_{m+1}) | \alpha_{m+1} \rangle \neq 0$, implying that $|\alpha_m\rangle$ and $|\alpha_{m+1}\rangle$ differ only on one pair of sites (i, j) , i.e. $|\alpha_{m+1}\rangle = a_i^\dagger a_j |\alpha_m\rangle$. This, along with the hard-core nature of the particles, implies that there is no intersection between any two worldlines. We can therefore conclude that a configuration ϕ can be uniquely identified as a *geometric braid* [30], and, as such, it represents an element of the braid group $\mathcal{B}_N(\mathcal{S})$ [31], where N is the particle number and \mathcal{S} is the surface in which the lattice is embedded. Two worldline configurations represent different braids or have different topological structures if it is impossible to continuously deform worldlines of one configuration into those of the other without cutting worldlines. On the other hand, configurations with the same topological structure represent the same braid. Therefore, the topological structure of ϕ is specified by how particles move *around* each other via sequential hopping $a_i^\dagger a_j$. A more rigorous definition of topological structure is given in the Supplemental Material, where we define topological structure based on homotopy rather than isotopy. To fix the idea, in Fig. 1, we show simple examples of worldline configurations and associated braid diagrams (i.e. the geometric representations of the braid group elements). Notice that different configurations can feature the same topological structure (panels (b) and (c)). Fig. 1 (d) shows how braids may easily become more complex as the number of particles is increased.

We now discuss how the topological structure of ϕ enters the ground-state expansion. We refer to [32] where authors estimate the level of chaos and correlations in a classical system by considering the topological structure of braids formed by particle trajectories. Here, we use geometric braids represented by configurations ϕ to study quantum correlations. Let $\mathcal{C}_\mathcal{T} \subset \mathcal{C}$ be the subset of configurations featuring the same topological structure \mathcal{T} (i.e. belonging to the same homotopy class). Eq. 1 allows one to restrict the integration domain to $\mathcal{C}_\mathcal{T}$ and introduce the state $|\Psi_\mathcal{T}\rangle = \sum_\alpha c_\alpha^\mathcal{T} |\alpha\rangle$ with:

$$|c_\alpha^\mathcal{T}|^2 = \langle \alpha | \Psi_\mathcal{T} \rangle \langle \Psi_\mathcal{T} | \alpha \rangle = \lim_{\beta \rightarrow \infty} \frac{1}{\mathcal{N}_\mathcal{T}} \int_{\phi \in \mathcal{C}_\mathcal{T} \cap \mathcal{C}_\alpha} \frac{\omega_\phi}{\mathcal{Z}_\beta} \quad (2)$$

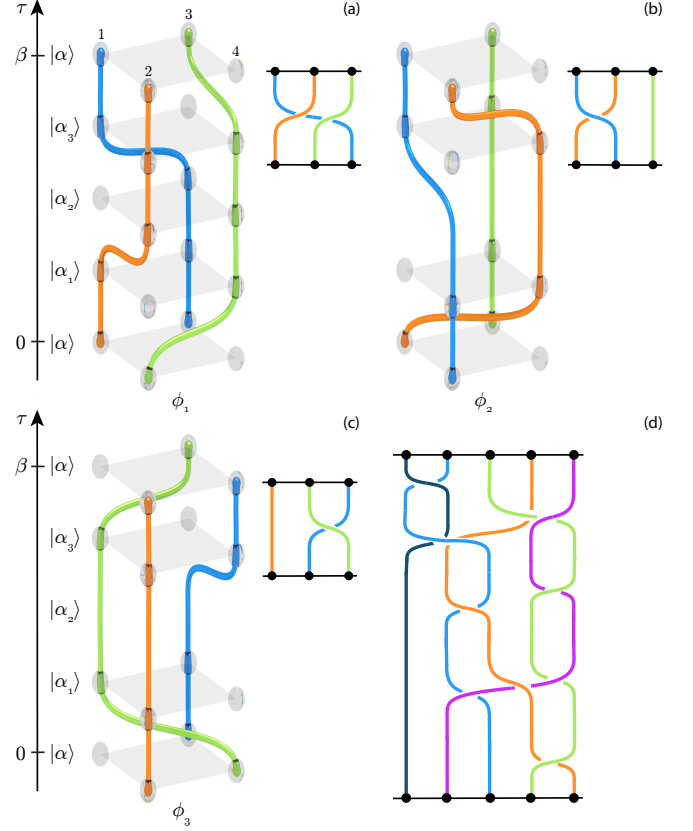


FIG. 1. Panels (a), (b) and (c): three examples of configurations of 3 particles on a 2×2 lattice. Configurations are collections of particle-paths in space and imaginary-time τ and are specified by a sequence of Fock states $|\alpha_i\rangle$ ordered in τ . The smaller figures represent geometric braids in 2D by only including the occupied sites. Particles are indistinguishable, colors are only meant to guide the eye. Panel (d): example of a more complex geometric braid involving 5 particles.

Here, $\mathcal{N}_\mathcal{T}$ is a normalizer. We define \mathcal{C}_{ϕ_i} as the subset of the configurations $\phi \in \mathcal{C}_\mathcal{T}$ with a fixed sequence $\phi_i = \{|\alpha\rangle, |\alpha_1\rangle, \dots, |\alpha_{n-1}\rangle, |\alpha\rangle\}$ or any cyclic permutation of the sequence that preserves the time-ordering. It follows that $\mathcal{C}_\mathcal{T}$ can be seen as the union of \mathcal{C}_{ϕ_i} , i.e. $\mathcal{C}_\mathcal{T} = \cup \mathcal{C}_{\phi_i}$, and that $(\cup \mathcal{C}_{\phi_i}) \cap \mathcal{C}^\alpha = \cup (\mathcal{C}_{\phi_i} \cap \mathcal{C}^\alpha)$. We can therefore split the integral in (2) as a sum of integrals on $\mathcal{C}_{\phi_i} \cap \mathcal{C}^\alpha$:

$$|c_\alpha^\mathcal{T}|^2 = \lim_{\beta \rightarrow \infty} \frac{1}{\mathcal{N}_\mathcal{T}} \sum_i \int_{\phi \in \mathcal{C}_{\phi_i} \cap \mathcal{C}^\alpha} \frac{\omega_\phi}{\mathcal{Z}_\beta} = \frac{1}{\mathcal{N}_\mathcal{T}} \sum_i w_\alpha^i. \quad (3)$$

where $w_\alpha^i = \int_{\phi \in \mathcal{C}_{\phi_i} \cap \mathcal{C}^\alpha} \frac{\omega_\phi}{\mathcal{Z}_\beta}$ if $|\alpha\rangle \in \phi_i$, and $w_\alpha^i = 0$ if $|\alpha\rangle \notin \phi_i$. Here, coefficient w_α^i can be interpreted as the collective weight of sequence ϕ_i . Using Eq. 3, one can see that the expansion coefficients $\{c_\alpha\}$ can be ‘re-arranged’ based on topological structure of configurations, therefore the topological structure may be encoding entanglement properties of the ground state. This can be understood as follows.

The multipartite entanglement of the groundstate $|\Psi\rangle$ is determined by which states $|\alpha\rangle$ have non-negligible $|c_\alpha|^2$, and, in the case of non-positive-definite $\{c_\alpha\}$, by the relative phase of the coefficients [5]. For positive-definite $\{c_\alpha\}$, as it is considered in this work, non-negligible $|c_\alpha|^2$ are closely related to non-negligible $\{\omega_\phi\}$. In other words, for any configuration ϕ containing state $|\alpha'\rangle$ in its sequence such that $c_{\alpha'} = \langle\alpha'|\Psi\rangle = 0$, $\omega_\phi \rightarrow 0$. This is a consequence of Eq. 1 with ω_ϕ positive-definite and the associated expression for ω_ϕ . Therefore, ϕ is relevant to the ground state only if *all* $|\alpha_m\rangle$ in ϕ contribute to the expansion of $|\Psi\rangle$.

This fact could result in the ability to differentiate different types of multipartite entanglement using topological structure of configurations. As an example, let us consider three insulating ground-states: checkerboard solid, valence bond solid, and \mathbb{Z}_2 spin liquid. Deep in the checkerboard solid, the ground state expansion is dominated by $|\alpha_{gs}\rangle$ [33] which corresponds to one of the two classical checkerboard configurations. Then, any relevant worldline configuration ϕ is expected to be either a trivial braid or a braid starting and ending at $|\alpha_{gs}\rangle$ with only few worldlines braided together locally. This ensures that Fock states in the sequence characterizing ϕ minimally differ from $|\alpha_{gs}\rangle$, i.e. they have almost the same occupation of bosons as $|\alpha_{gs}\rangle$. Deep in the valence bond solid at filling 1/3 on Kagome lattice [34], the ground state expansion is dominated by Fock states corresponding to the classical hexagon-solid-backbone of holes with only isolated hexagons harboring local fluctuations of occupation numbers of bosons. Therefore, relevant ϕ may only have few worldlines braided together. These worldlines prevalently start and end on the hexagons where local resonances exist. Finally, in the \mathbb{Z}_2 spin liquid on Kagome lattice, the ground state is an expansion that includes Fock states which can be dramatically different from each other in terms of occupation number of bosons. Nonetheless, every pair of states entering the expansion can be connected by sequential operations of the form $a_i a_j^\dagger$ [35] with small energy cost. Hence, deep in this phase, there can be relevant ϕ such that very different states (in terms of bosonic occupation number) appear in the sequence characterizing ϕ . As a consequence, one may expect that, unlike in CB and VBS, complex non-local braids connecting these states may appear in the configuration.

Note that, there may be more than one ϕ characterized by the same collection of states (not necessarily in the same time-sequence) but with different ω_ϕ . Each such ϕ corresponds to a certain way in which quantum fluctuations (i.e. $a_i a_j^\dagger$ operations) connect the set of states in ϕ . Therefore, $\{\omega_\phi\}$ may realize a more comprehensive deciphering of the entanglement of $|\Psi\rangle$ than $\{c_\alpha\}$, and relevant ϕ can be interpreted as a visualization of the generation of quantum fluctuation which essentially gives rise to the entanglement.

Numerical results The simplest topological invariant that can be used to (partially) characterize the topological structure of configurations is the statistics of permutation cycles [36, 37]. Permutation cycles are obtained by gluing together worldlines at imaginary time $\tau = \beta$ and $\tau = 0$. Their length is proportional to the *minimal* number of braiding events occurring between worldlines participating in a cycle and does not detect braiding events among different permutation cycles. Hence, the length of permutation cycles does not provide a complete characterization of a topological structure.

We use the topological invariant $\vec{q}_\phi = (n_1, n_2, \dots, n_N)$, where n_l is the number of permutation cycles of length $\lambda = l \times \beta$ appearing in the configuration, and N is the total number of particles. For example, configurations in Fig. 1 are characterized by $\vec{q}_{\phi_1} = (0, 0, 1)$ and $\vec{q}_{\phi_2} = \vec{q}_{\phi_3} = (1, 1, 0)$. By collecting statistics on \vec{q}_ϕ , one can compute the probability that topological structures characterized by \vec{q}_ϕ appear:

$$p_{\vec{q}} = \int_{\phi \in \mathcal{C}_{\vec{q}}} \frac{\omega_\phi}{Z_\beta}, \quad (4)$$

where $\mathcal{C}_{\vec{q}}$ is the set of all configurations characterized by the same topological invariant \vec{q}_ϕ (these configurations do not necessarily have the same topological structure). We calculate probability $p_{\vec{q}}$ for all \vec{q}_ϕ measured and obtain a probability distribution that can be interpreted as a *topological spectrum* capable of fingerprinting different ground-states with different entanglement properties.

We perform quantum Monte Carlo simulations of the extended Bose Hubbard model:

$$H = -t \sum_{\langle ij \rangle} a_i^\dagger a_j + H_0 \quad (5)$$

where H_0 is the diagonal part of H in the Fock basis and $\langle ij \rangle$ refers to sum over nearest neighbors. Here we choose hopping $t > 0$ to guarantee that ground-state coefficients c_α are positive-definite (see also Supplemental Material). We consider four H_0 : (1) $H_0 = V \sum_{\langle ij \rangle} n_i n_j$ in a square lattice which, at filling factor 1/2, can stabilize a CB and a SF phase [33]; (2) $H_0 = V \sum_{ij} \frac{n_i n_j}{r_{ij}^3}$ in a square lattice which, among others, stabilizes a STR phase at filling factor 1/3 [38] (here, r_{ij} is the distance between site i and j and we set a cut-off to $r_{ij} = 4$); (3) $H_0 = V \sum_{\odot} n_i n_j$, where the sum over \odot refers to the sum between sites on the same hexagon of the Kagome lattice, which, at filling factor 1/2 and 1/3 can stabilize a SF and a \mathbb{Z}_2 topologically ordered phase [13, 39]; (4) $H_0 = V \sum_{\langle ij \rangle} n_i n_j$ on the Kagome lattice, which at 1/3 stabilizes a valence bond solid (VBS) [34]. For all models we consider periodic boundary conditions. We measure topological invariant \vec{q}_ϕ for a number of configurations of the order of 10^4 to 10^5 . From these measurements, we compute $p_{\vec{q}}$.

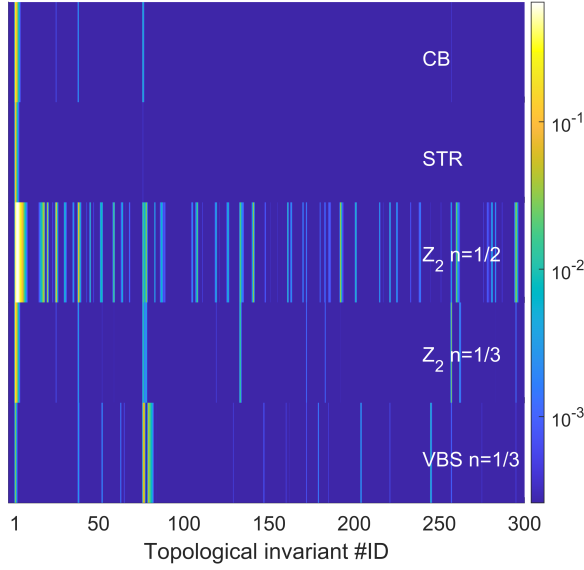


FIG. 2. Distribution $p_{\tilde{j}}$ of ground-states of different insulating quantum phases for comparable system-sizes (in terms of total number of sites): $L = 10$ for square lattice and $L = 6$ unit cells for Kagome lattice. From top to bottom: CB at $V/t = 20$, STR at $V/t = 60$, \mathbb{Z}_2 for $n = 1/2$ and $n = 1/3$ at $V/t = 15$, and VBS at $V/t = 15$. Inverse temperature $\beta/t = 18$.

As shown in Fig. 2, where we plot the topological spectrum corresponding to each ground-state of the insulating phases, ground-states corresponding to different multipartite entanglement manifest visible differences in their topological signatures. The color-map represents $p_{\tilde{j}}$ as function of a label of all topological invariants found. We label them according to their average permutation-cycles's length by excluding 1β -long permutation cycles (see Supplemental Material for details). We plot the topological spectra of CB at $V/V_c = 10$, STR at $V/V_c = 4$, and \mathbb{Z}_2 and VBS at $V \approx 2V_c$. We observe that these ground-states are characterized by topological invariants that feature small permutation cycles, as expected for insulating phases, with the majority of worldlines in 1β permutation cycles and a few worldlines mainly participating to 2β and/or 3β permutation cycles. Longer permutation cycles such as 4β and 5β only appear in ground-states of VBS and \mathbb{Z}_2 phases. See table in Supplemental Material for details.

We also looked at how the complexity of topological structures changes with system size. We quantified the complexity by measuring f_{PC} the fraction of particles in permutation cycles longer than 1β (see Fig. 3). We found that deep in the CB and STR phases ($V/V_c = 10$ and $V/V_c \approx 4$), f_{PC} does not change as L is increased. This is not surprising, since deep in these phases, one expects a 'simple' multipartite entanglement, as discussed

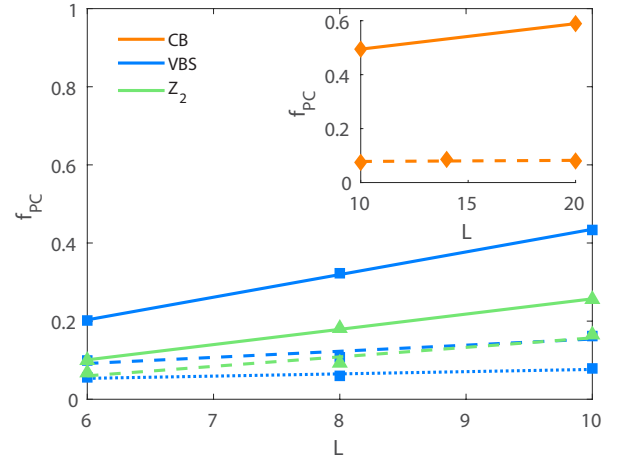


FIG. 3. Fraction of particles in permutation cycles longer than $1/\beta$ as a function of system size L for CB, VBS and \mathbb{Z}_2 ground states. CB at $V/V_c = 1.7$ ($V/V_c = 10$) continuous (dashed) line; VBS at $V/V_c = 2$ (continuous), $V/V_c = 3$ (dashed) and $V/V_c = 4$ (dotted); \mathbb{Z}_2 at $V/V_c = 2$ (continuous) and $V/V_c = 3$ (dashed).

in the Supplemental Material. This is no longer true as one gets closer to the transition to the SF phase. Here, the complexity of the topological structure increases with L . Larger L implies a larger Hilbert space which leads to a more complex ground-state expansion (and entanglement). A similar observation is valid for the VBS. While f_{PC} increases with L at $V/V_c = 2$ (solid blue line), this trend becomes less pronounced as V/V_c is increased and at $V/V_c = 4$ (dotted blue line) the L -dependence of f_{PC} has become minimal. The situation for the \mathbb{Z}_2 phase at $1/3$ filling seems more complex. At $V/V_c = 2$ (solid green line), we observe a strong L -dependence of f_{PC} . As V/V_c is increased to 3 (dashed green line), the L -dependence remains relatively pronounced and certainly more pronounced than in the VBS case at the same value of V/V_c . This poses an interesting question as whether the L -dependence of f_{PC} for the \mathbb{Z}_2 case is only affected by the distance from the transition point with the SF phase, or it also depends on the fact that the \mathbb{Z}_2 ground-state is expected to still retain more complex braids deeper in the phase, as previously discussed.

Conclusions We have proposed a new perspective to study multipartite entanglement in hardcore bosonic systems by considering worldline configurations (resulting from the path-integral formulation) as geometric braids. The set of weights of these configurations fully encodes the ground-state properties. This proposal has its roots in the fact that a worldline configuration can be seen as a representation of a certain way in which quantum fluctuations connect a Fock state to itself through a sequence of states. Moreover, the geometric-braid nature of the set of particle trajectories in a configuration attributes a topological description to quantum fluctuations. Hence, con-

sidering that the ground-state entanglement can be seen as originating from the quantum fluctuations induced by the hopping, we expect that properties (e.g. topological properties) of worldline configurations may decipher multipartite entanglement properties of the ground state. Using quantum Monte Carlo simulations, we tested this idea by assigning a “topological spectrum” to ground-states in the checkerboard, stripe, valence-bond solids, \mathbb{Z}_2 topologically ordered spin liquid, and superfluid phase. We find that the “spectrum” can be used to distinguish these ground states.

ACKNOWLEDGEMENTS

The authors wish to thank Lorenza Viola and Vittorio Penna for fruitful discussions. F.L. and B.C.S. thank Alejandra Rosselli, Ben Roque and Brett Laramée for useful suggestions on local measurements of STR phases. W.W. thanks Anne E. B. Nielsen and Yi Li for motivation on considering topological properties of worldline configurations.

* flingua@clarku.edu

- [1] R. Horodecki and K. Horodecki, *Rev. Mod. Phys.* **81**, 865 (2009).
- [2] C. T. Asplund, A. Bernamonti, F. Galli, and T. Hartman, *J. High Energy Phys.* **09**, 110 (2015).
- [3] L. E. Fermi, L. Pezzè, M. Gabbriellini, L. Lepori, and A. Smerzi, *Phys. Rev. Lett.* **119**, 250401 (2017).
- [4] D. A. Abanin and I. Bloch, *arXiv:1804.11065v2* (2019), *arXiv:arXiv:1804.11065v2*.
- [5] B. Zeng, X. Chen, D.-L. Zhou, and X.-G. Wen, *Quantum Information Meets Quantum Matter – From Quantum Entanglement to Topological Phase in Many-Body Systems* (Springer-Verlag New York, 2019) pp. XXII, 364.
- [6] P. J. Love, A. M. van den Brink, A. Y. Smirnov, M. H. S. Amin, M. Grajcar, E. Il’ichev, A. Izmailkov, and A. M. Zagorskin, *Quantum Information Processing* **6**, 187 (2007).
- [7] M. Hofmann, A. Osterloh, and O. Gühne, *Phys. Rev. B* **89**, 134101 (2014).
- [8] B. Jungnitsch, T. Moroder, and O. Gühne, *Phys. Rev. Lett.* **106**, 190502 (2011).
- [9] X. Chen, Z. C. Gu, and X. G. Wen, *Phys. Rev. B* **82**, 155138 (2010).
- [10] A. Kitaev and J. Preskill, *Phys. Rev. Lett.* **96**, 110404 (2006), *arXiv:0510092 [hep-th]*.
- [11] M. Levin and X. G. Wen, *Phys. Rev. Lett.* **96**, 110405 (2006).
- [12] L. Balents, *Nature* **464**, 199 (2010).
- [13] S. V. Isakov, M. B. Hastings, and R. G. Melko, *Nature Physics* **7**, 772 (2011).
- [14] H.-C. Jiang, Z. Wang, and L. Balents, *Nature Physics* **8**, 902 (2012).
- [15] J. Eisert, M. Cramer, and M. B. Plenio, *Rev. Mod. Phys.* **82**, 277 (2010), *arXiv:0808.3773*.
- [16] J. T. Barreiro, P. Schindler, O. Gühne, T. Monz, M. Chwalla, C. F. Roos, M. Hennrich, and R. Blatt, *Nature Physics* **6**, 943 EP (2010).
- [17] P. Hauke, M. Heyl, L. Tagliacozzo, and P. Zoller, *Nature Physics* **12**, 778 EP (2016).
- [18] M. Gabbriellini, A. Smerzi, and L. Pezzè, *Scientific Reports* **8**, 15663 (2018).
- [19] I. Frérot and T. Roscilde, *Nature Communications* **10**, 577 (2019).
- [20] H. Kampermann, O. Gühne, C. Wilmott, and D. Bruß, *Phys. Rev. A* **86**, 032307 (2012).
- [21] S. T. Flammia, A. Hamma, T. L. Hughes, and X.-G. Wen, *Phys. Rev. Lett.* **103**, 261601 (2009).
- [22] F. Verstraete, J. Dehaene, B. De Moor, and H. Verschelde, *Phys. Rev. A* **65**, 052112 (2002).
- [23] J. I. Cirac and F. Verstraete, *J. Phys. A Math. Theor.* **42**, 504004 (2009).
- [24] N. Schuch, I. Cirac, and D. Pérez-García, *Ann. Phys. (N. Y.)* **325**, 2153 (2010), *arXiv:1001.3807*.
- [25] S. Yang, T. B. Wahl, H. H. Tu, N. Schuch, and J. I. Cirac, *Phys. Rev. Lett.* **114**, 106803 (2015).
- [26] S. Haddadi and M. Bohloul, *International Journal of Theoretical Physics* **57**, 3912 (2018).
- [27] R. Feynman, *Statistical mechanics: a set of lectures (advanced book classics)* (Avalon Publishing, New York, 1998).
- [28] L. H. Kauffman and S. J. Lomonaco Jr, *New Journal of Physics* **4**, 73 (2002).
- [29] G. Alagic, M. Jarret, and S. P. Jordan, *Journal of Physics A: Mathematical and Theoretical* **49**, 075203 (2016).
- [30] C. Kassel and V. Turaev, *Graduate texts in mathematics ; 82* (Springer-Verlag New York, 2008) pp. X, 338.
- [31] J. R. T. de Lima, *arXiv:1811.02006* (2018), *arXiv:1811.02006*.
- [32] J.-L. Thiffeault, *Chaos: An Interdisciplinary Journal of Nonlinear Science* **20**, 017516 (2010).
- [33] F. Hébert, G. G. Batrouni, R. T. Scalettar, G. Schmid, M. Troyer, and A. Dorneich, *Phys. Rev. B* **65**, 014513 (2001).
- [34] S. V. Isakov, S. Wessel, R. G. Melko, K. Sengupta, and Y. B. Kim, *Phys. Rev. Lett.* **97**, 147202 (2006).
- [35] W. Wang and B. Capogrosso-Sansone, *Scientific Reports* **7**, 11071 (2017).
- [36] R. P. Feynman, *Physical Review* **91**, 1291 (1953).
- [37] D. Ceperley, *Rev. Mod. Phys.* **67**, 279 (1995).
- [38] B. Capogrosso-Sansone, C. Trefzger, M. Lewenstein, P. Zoller, and G. Pupillo, *Physical review letters* **104**, 125301 (2010).
- [39] K. Roychowdhury, S. Bhattacharjee, and F. Pollmann, *Phys. Rev. B* **92**, 075141 (2015).

Supplemental Material: A topological signature of multipartite entanglement

F. Lingua^{†,1,*} W. Wang^{†,2} L. Shpani,¹ and B. Capogrosso-Sansone¹

¹*Department of Physics, Clark University, Worcester, Massachusetts 01610, USA*

²*Max Planck Institute for the Physics of Complex Systems, Nöthnitzer Str. 38, 01187 Dresden, Germany*

[†]*These authors contribute equally to the work.*

(Dated: December 5, 2019)

REVIEW OF PATH-INTEGRAL FORMALISM

The imaginary-time path-integral formulation of the density matrix ρ is the foundation of path integral Monte Carlo (PIMC) algorithms. Here, we consider lattice hard-core bosons in two dimensions. Let us define $|\alpha\rangle = |0, 1, \dots\rangle$, where 1 corresponds to occupation of a hard-core boson and 0 to no occupation in the Fock basis. The generic Bose-Hubbard-type model describing the system has the form:

$$H = - \sum_{(i,j)} (t_{ij} a_i^\dagger a_j + \text{H.c.}) + H_0 \quad (1)$$

where the first term is the hopping between site i and j with strength t_{ij} (in the following denoted by H_1), while the second term is an arbitrary diagonal term, e.g., $\sum_{(i,j)} V_{ij} a_i^\dagger a_i a_j^\dagger a_j$. Model (1) conserves the number of particles. In this work, we work at fixed filling factor and consider $t_{ij} > 0$.

Within the path-integral formalism [1–3], the partition function at temperature $k_B T = 1/\beta$

$$\mathcal{Z}_\beta = \text{Tr} e^{-\beta H} = \sum_\alpha \langle \alpha | e^{-\beta H} | \alpha \rangle = \int_{\phi \in \mathcal{C}} \omega_\phi, \quad (2)$$

is an integral of weights ω_ϕ of worldline configurations (see below for more details), where ϕ is a combination of continuous and discrete indexes which uniquely specifies the configuration, and \mathcal{C} is the set of all configurations. A configuration ϕ is a collection of worldlines (see Fig. 1 in main text) where each worldline represents the path of a particle in imaginary-time and space. In the interaction picture, ϕ is specified by a sequence of imaginary time instants at which single hopping events happen $0 < \tau_1 < \dots < \tau_{n-1} < \beta$, and the corresponding sequence of Fock states $\{|\alpha\rangle, |\alpha_1\rangle, \dots, |\alpha_{n-1}\rangle, |\alpha\rangle\}$, where state $|\alpha_i\rangle$ is the state at time τ_i . Note that, by definition of \mathcal{Z}_β , periodic boundary conditions in imaginary time hold, that is, the configuration starts and ends with the same occupation of lattice sites specified by a Fock state $|\alpha\rangle$. Within this framework, weights ω_ϕ can be expressed as [1–3]:

$$\omega_\phi \propto \langle \alpha | H_1(\tau_1) | \alpha_1 \rangle \cdots \langle \alpha_n | H_1(\tau_n) | \alpha \rangle. \quad (3)$$

Note that, due to periodic boundary conditions in time, any cyclic permutation of $\{|\alpha_i(\tau_i)\rangle\}$ results in the same configuration ϕ (with a different choice of $\tau = 0$). The

expectation value of a thermodynamic observable O is $\langle O \rangle_\beta = \int_{\phi \in \mathcal{C}} \frac{\omega_\phi O_\phi}{\mathcal{Z}_\beta}$ where $\omega_\phi/\mathcal{Z}_\beta$ is a probability density and O_ϕ is the value of O in configuration ϕ .

Here, we only consider models with $t_{ij} > 0$ for which the ground-state of a finite-size system is unique and has positive expansion coefficients on Fock states $|\alpha\rangle$ (see below). Let us denote the subcollection of configurations ϕ starting and ending at $|\alpha\rangle$ by \mathcal{C}^α . Then, properties of ground-state $|\Psi\rangle$, as determined by $c_\alpha = \langle \alpha | \Psi \rangle$, are completely encoded in the integrals

$$\langle \alpha | \Psi \rangle \langle \Psi | \alpha \rangle = \lim_{\beta \rightarrow \infty} \langle \alpha | \frac{e^{-\beta H}}{\mathcal{Z}_\beta} | \alpha \rangle = \lim_{\beta \rightarrow \infty} \int_{\phi \in \mathcal{C}^\alpha} \frac{\omega_\phi}{\mathcal{Z}_\beta}. \quad (4)$$

This means that ground-state properties, such as entanglement and quantum correlations, can be equivalently inferred from $\{\omega_\phi\}$ rather than $\{c_\alpha\}$.

UNIQUENESS AND POSITIVITY OF THE GROUND-STATE

The uniqueness and positivity of the ground-state can be shown using a simplified version of the argument used in Ref. [4]. The argument is based on the irreducibility of the hopping matrix which, by Perron-Frobenius theorem, guarantees the uniqueness and positivity of the expansion coefficients of the ground-state. As proved in Ref. [4], irreducibility is a consequence of the fact that any two Fock states $|\alpha\rangle$ and $|\alpha'\rangle$ can be connected by sequentially applying $a_i^\dagger a_j$. This is trivial if the lattice is connected as it is generally assumed.

DEFINITION OF TOPOLOGICAL STRUCTURE

We characterize the topological structure of geometric braids by homotopy on them rather than isotopy (on which the standard definition of the braid group is based). While in both cases topologically-equivalent geometric braids can be continuously deformed into each other, isotopy further requires the “ends” (i.e state $|\alpha\rangle$ in configurations) of topologically equivalent geometric braids to be fixed. Here, we do not need this additional constraint because, due to periodic boundary conditions in imaginary time, $|\alpha\rangle$ has no special meaning in the sequence of states specifying a certain configuration. In

other words, any configuration corresponding to a cyclic permutation of a given sequence of states has exactly the same weight.

LABELLING OF TOPOLOGICAL STRUCTURES

In general, configurations belonging to different ground-states correspond to geometric braids that cannot be compared between each other as the number N of particles required to stabilize these phases may be different from case to case. In other words, they belong to different braiding groups $\mathcal{B}_N(\mathcal{S})$. However, since in insulating ground-states the $1/\beta$ -long permutation cycle (PC) is always macroscopically occupied, one may only consider the geometric braids between the N' particles that do not participate in the $1/\beta$ -long PC. This can be done by first redefining topological invariant \vec{q}_ϕ as

$$\vec{p}_\phi = (\dots, n_l \times l \dots) / N, \quad (5)$$

so that component l of \vec{p}_ϕ is the fraction of particles (worldlines) involved in permutation cycles of length l . Next, we introduce a new topological invariant $\vec{p}'_\phi = (2 \times n_2, 3 \times n_3 \dots N \times n_N) / N$ (note that the $1/\beta$ long PC is not included) corresponding to geometric braids belonging to $\mathcal{B}_{N'}(\mathcal{S})$. By only considering the fraction of particles involved in PC longer than $1/\beta$, it is possible to better compare the arrangement of permutation cycles in different ground-states.

Finally, we introduce a topological invariant which can be interpreted as an ‘average’ length of PC useful to order and label different \vec{p}_ϕ :

$$\langle \lambda_\phi \rangle = \vec{p}'_\phi \cdot \vec{\lambda} \quad (6)$$

where $\vec{\lambda} = (2, \dots, N)$ is the vector of PC lengths and symbol \cdot refers to dot product. Topological spectra shown in Fig. 2 of the main text and Fig. 2 here are organized according to (6).

TOPOLOGICAL SIGNATURES IN INSULATING GROUND-STATES

In the table of Fig. 1 we sketch the most probable (with a probability greater than 0.01) arrangement of permutation cycles (first column) for the insulating phases, with corresponding probability to appear in the ground-state expansions (remaining columns). Each arrangement of permutation cycles is represented in terms of the fraction of worldlines (percentages under the braid diagrams) participating to the corresponding permutation cycle: $1/\beta$ -long PC corresponding to straight worldlines (blue), $2/\beta$ -long PC corresponding to two worldlines braiding together (orange), $3/\beta$ -long PC and longer corresponding to three or more worldlines braiding together (green, violet and brown for $3/\beta$, $4/\beta$ and $5/\beta$ respectively).

TOPOLOGICAL SIGNATURES IN SUPERFLUID GROUND-STATES

In Fig. 2, we plot the spectrum of the SF ground-state. As expected, we notice the presence of topological invariants with large permutation cycle average length. Often times, configurations are such that most worldlines participate to the same permutation cycle. In Fig. 2, we also sketch some of the most probable permutation cycle lengths. The percentages in the sketches represent the fraction of particles involved in the permutation cycles.

LOCAL MEASUREMENTS AND INFORMATION IN CHECKERBOARD AND STRIPE PHASES

Here, we discuss how local measurements of occupation number(s) (i.e. binary measurements of $n_i = 0, 1$) in CB and STR phases can extract information on the entire system. In the limit $V/t \rightarrow \infty$ the true ground-states [5] of CB and STR phases are given by:

$$|\Psi_{CB}\rangle = \frac{|\text{Checkerboard 1}\rangle + |\text{Checkerboard 2}\rangle}{\sqrt{2}} \quad (7)$$

$$|\Psi_{STR}\rangle = \frac{|\text{Stripe 1}\rangle + |\text{Stripe 2}\rangle + |\text{Stripe 3}\rangle + |\text{Stripe 4}\rangle + |\text{Stripe 5}\rangle + |\text{Stripe 6}\rangle}{\sqrt{6}} \quad (8)$$

The CB ground-state is described by the standard GHZ state in (7), and it is straightforward to show that measuring the occupation number of a single lattice site is sufficient to determine the state in which the system collapses. Indeed, the information content of $|\Psi_{CB}\rangle$ is 1 bit so that the measurement of a single site is enough. On the other hand, in the STR case, the choice of local measurements is not as obvious. Being $|\Psi_{STR}\rangle$ the superposition of six states, one expects that a measurement of 3 sites is sufficient to distinguish between the six cases. Indeed, the information content of $|\Psi_{STR}\rangle$ is $I = -\sum_i p_i \log_2(p_i) = \log_2 6 \simeq 2.58$ bits, where $p_i = 1/6$ is the probability of each state in the ground-state expansion. In order to differentiate the six cases, one can engineer a simple algorithm involving a minimal number of lattice sites. This algorithm is not unique. We give an example in Fig. 3, where we schematically depict the flowchart of the algorithm. In two cases (C and D) two measurements (2 bits) are sufficient to determine the state in which the system has collapsed, while in the remaining four cases (A, B, E, and F) three measurements (3 bits) are required. This results in an average information of $2 \times \frac{1}{3} + 3 \times \frac{2}{3} \simeq 2.67$ bits processed by the algorithm which therefore efficiently measure the information content of $|\Psi_{STR}\rangle$.

This discussion shows that, in both cases, performing local measurements is sufficient to extract information

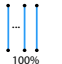
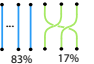
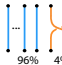
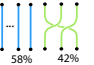
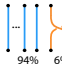
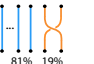
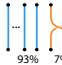
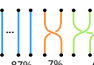
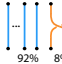
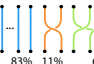
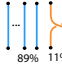
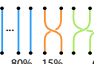
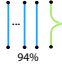
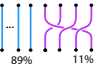
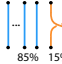
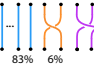
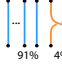
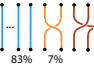
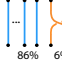
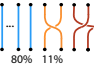
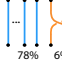
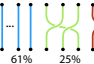
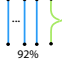
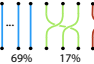
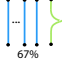
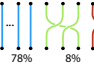
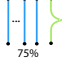
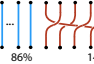
	CB	STR	VBS n=1/3	\mathbb{Z}_2 n=1/3	\mathbb{Z}_2 n=1/2		CB	STR	VBS n=1/3	\mathbb{Z}_2 n=1/3	\mathbb{Z}_2 n=1/2
	0.61	0.80	0.20	0.55	0.02		-	-	0.19	-	-
	0.29	0.18	-	-	0.08		-	-	0.01	-	-
	-	-	0.01	0.25	-		-	-	-	-	0.03
	-	-	-	-	0.12		-	-	-	-	0.04
	0.06	0.02	-	-	-		-	-	-	-	0.03
	-	-	-	0.05	0.11		-	-	-	-	0.02
	0.01	-	0.02	-	-		-	-	-	0.06	-
	-	-	-	-	0.07		-	-	-	0.03	-
	-	-	-	-	0.03		-	-	-	-	0.02
	-	-	0.01	-	-		-	-	-	-	0.02
	-	-	0.01	-	-		-	-	-	0.02	-
	-	-	0.18	0.02	-		-	-	-	0.04	-
	-	-	0.04	-	0.07		-	-	-	0.05	-
	-	-	0.11	-	-		-	-	-	0.03	-

FIG. 1. Arrangement of permutation cycles in ground-states of different insulating quantum phases. Numbers in the table represents the probability of each arrangement to appear in the related phase. The percentage in the diagrams refers to the components of \vec{p}_ϕ (5) (i.e. the fraction of particles participating in permutation cycles of that length). CB for $L = 10$ and $V/t = 20$; STR for $L = 12$ and $V/t = 20$; VBS at $n = 1/3$ for $L = 6$ unit cells and $V/t = 30$; \mathbb{Z}_2 at $n = 1/3$ and $n = 1/2$ for $L = 6$ unit cells and $V/t = 15$.

on the whole system revealing the simplicity of the multipartite entanglement in CB and STR phases.

* flingua@clarku.edu

[1] E. Pollock, Phys. Rev. B **30**, 2555 (1984).

[2] D. Ceperley, Rev. Mod. Phys. **67**, 279 (1995).

[3] F. Lingua, B. Capogrosso-Sansone, A. Safavi-Naini, A. Ja-

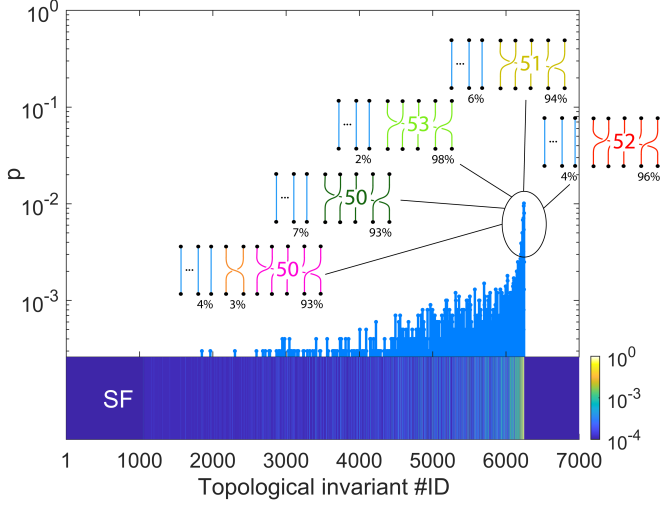


FIG. 2. Distribution $p_{\tilde{T}}$ of the ground-state of a superfluid phase on Kagome lattice ($V/t = 5$, $n = 1/2$). Top panel shows the five most likely topological invariants. Percentages below the geometric braids represent the fraction of particles involved in permutation cycles of that length.

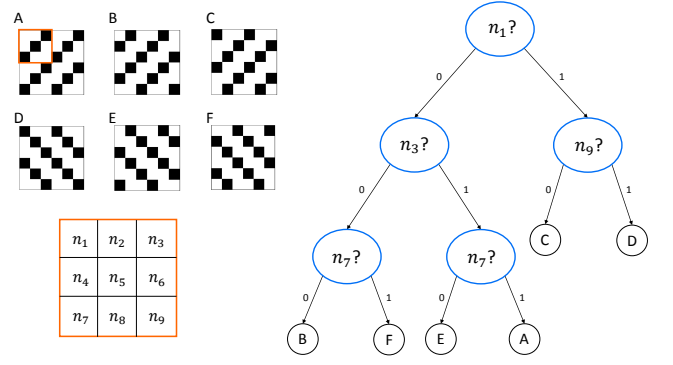


FIG. 3. Algorithm to determine the configuration of the STR phase by means of local measurement of site occupation numbers n_i .

- hangiri, and V. Penna, *Physica Scripta* **93**, 105402 (2018).
 [4] W. Wang, V. Penna, and B. Capogrosso-Sansone, *Phys. Rev. E* **90**, 022116 (2014).
 [5] B. Zeng, X. Chen, D.-L. Zhou, and X.-G. Wen, *Quantum Information Meets Quantum Matter – From Quantum Entanglement to Topological Phase in Many-Body Systems* (Springer-Verlag New York, 2019) pp. XXII, 364.